

Measurements of Top quark pair production cross section and Search for Resonances at Tevatron

Roberto Rossin^{*†}

*University of Florida - Fermilab - P.O.Box 500 - MS 318
60510, Batavia IL (USA)
E-mail: rossin@fnal.gov*

We present the measurement of the top pair production cross-section at Tevatron in p-pbar collisions at 1.96 TeV. We also compare selected kinematical distributions with the predictions of the Standard Model.

In the dilepton mode, we select events with two charged leptons, high missing transverse energy and at least 2 jets.

In the lepton+jets mode, we select events with one charged lepton, high missing transverse energy and at least 3 jets. We present several complementary measurements using kinematic discrimination and/or *b*-tagging.

In the all-hadronic channel, we select events with ≥ 6 jets and ≤ 8 jets. We present a measurement using an optimized kinematic selection and events with one or more displaced secondary vertices.

We also report on the search for non-standard model resonance states in the invariant mass spectrum of top pairs in lepton+jets events. We present two complementary measurements, one adopts an event reconstruction technique that uses matrix element informations to increase the sensitivity for discovery, the other performs a constrained kinematic fit and requires *b*-tagging.

*International Workshop on Top Quark Physics
January 12-15, 2006
Coimbra, Portugal*

^{*}Speaker.

[†]On Behalf of the CDF and D \emptyset collaborations

1. Introduction

Since the discovery of the top quark in 1995 by CDF and D \emptyset collaborations[1] an extensive program to characterize this particle is underway. The top is by far the heaviest among the quark family and offers a new testing ground for the standard model, including quantum chromodynamics; due to its large mass the top quark is the entity that is most strongly coupled to the symmetry-breaking dynamics and then play as a powerful probe in this physics sector.

The top quark production cross section measurements by CDF and D \emptyset experiments can be considered as the first step toward exploiting this sector but also provide a test bench for tools and techniques which will be useful for physics analysis at the LHC.

According to the standard model, top quark pair production at the Tevatron ($\sqrt{s} = 1.96$ TeV) proceeds via quark-antiquark annihilation (85%) and gluon fusion (15%), with a NLO cross section of $6.7^{+0.9}_{-0.7}$ pb for $M_{top} = 175$ GeV/c².

Besides the standard model $t\bar{t}$ production, other production mechanisms have been proposed. The existence of a narrow vector resonances decaying to $t\bar{t}$ has been predicted by theoretical models like the top-color-assisted technicolor [2, 3]. This model accounts for the spontaneous electroweak symmetry breaking by introducing a new strong dynamics which would explain the large top quark mass.

Unitarity constraints on the CKM matrix require the top quark to decay to a W boson and a b quark, so the W decays (either $W \rightarrow \ell\nu$ or $W \rightarrow q\bar{q}$) define the signature for the $t\bar{t}$ events.

Figure 1 shows the breakdown of each type of final state; the final states containing τ leptons have been kept separated since the τ immediately decays and cannot be easily identified. The three main final states available for the analysis are thus: dilepton, lepton plus jets, all hadronic; all of them have jets in the final state, dileptonic and lepton plus jets channels have also isolated high- p_T leptons and large W⁻ missing transverse energy (\cancel{E}_T) due to the escaping neutrinos. While the isolated tracks are reliably identified and reconstructed by the tracking and calorimetric apparatus, the jet reconstruction and energy measurement, the \cancel{E}_T measurement and the identification of the b-jets (*b-tagging*) require sophisticated tools developed [4, 5] to obtain precise event reconstruction, background rejection and determination of the data sample composition.

2. Top Pair Production Cross Section

Both the CDF and D \emptyset experiments [6, 7, 8] measure the $t\bar{t}$ production cross section in all three final states either performing counting experiments or by fitting the data to kinematical distributions that can discriminate signal from background.

Performing the analyses in the three channels allows to reduce the uncertainty by combining the

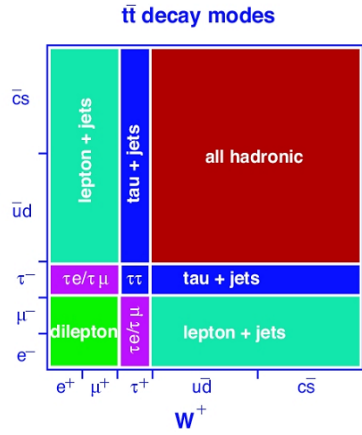


Figure 1: $t\bar{t}$ decay channels.

measurements, but also provides a consistency check across the channel and then tests for the presence of physics beyond the standard model (e.g. $t \rightarrow H^+ b$) which modifies the balance among the channels.

2.1 Dilepton channel

Top dilepton events, in which both W's decay to an electron or muon and a ν , are characterized by two high- p_T leptons, large missing transverse energy (\cancel{E}_T) due to the escaping neutrinos, and two jets from the b quarks. This channel is the cleanest ($S/B \sim 1.5 - 3$) but also the one with the smallest statistics (5% branching ratio for the e/ μ analyses) among the three final states. The main contributions to backgrounds come from Drell-Yan production, $W \rightarrow \ell\nu + jets$ events where a jet is misidentified as a lepton and diboson (WW, WZ and ZZ) production. Different approaches are adopted to measure the cross section in this channel.

D \emptyset collaboration performed a counting experiment in a data sample of approximately 370 pb^{-1} . After requiring two opposite charge leptons and two jets, different sets of cuts have been applied to reject the backgrounds for the three channels (e^+e^- , $e^\pm\mu^\mp$, $\mu^+\mu^-$). The large \cancel{E}_T is used to discriminate the ($\ell\ell$) signal from the $Z/\gamma^* \rightarrow \ell\ell$ backgrounds while on the $e^\pm\mu^\mp$ channel the largest background, which arises from $Z \rightarrow \tau^+\tau^-$, is suppressed by requiring large scalar transverse energy ($H_T^\ell = p_T^{\ell_1} + \sum p_T^j$, where $p_T^{\ell_1}$ denotes the p_T of the leading lepton). The cross section measurement has been performed in the three channels by counting the background subtracted signal and correcting for the detector acceptance and reconstruction efficiencies (Fig. 2). The average cross section obtained is $\sigma_{t\bar{t}} = 8.6^{+2.3}_{-2.0}(\text{stat})^{+1.2}_{-1.0}(\text{syst}) \pm 0.6(\text{lumi}) \text{ pb}$.

Given the limited statistics of the dilepton sample, a natural choice is to increase acceptance by loosening the selection cuts. Following this idea CDF performed a counting experiment analysis in a 360 pb^{-1} data sample. Two opposite-charged, high p_T lepton candidates are required, the first one has to pass strict tracking and calorimetric requirements, while for the second one only tracking selections are applied. This allows to recover acceptance from partially instrumented regions of the detector and to accept also single prong τ hadronic decay. Events with zero or one jets are studied to test the background predictions and events with two or more jets are used to calculate the cross section (Fig. 3). The measured cross section is: $\sigma_{t\bar{t}} = 10.1 \pm 2.2(\text{stat}) \pm 1.4(\text{syst}) \text{ pb}$.

A different approach with respect to the counting experiments take advantage of the different kinematic behavior of the $t\bar{t}$ events if compared to the background processes in the two-dimensional \cancel{E}_T and jet multiplicity space. Data are fit to extract the contributions from $t\bar{t}$, WW and $Z \rightarrow \tau\tau$. The strength of this approach lies in the very different regions of $\cancel{E}_T - N_{jet}$ space occupied by the standard model processes contributing to the high- p_T dilepton sample. The measurement carried out at CDF with 200 pb^{-1} of data gives: $\sigma_{t\bar{t}} = 8.6^{+2.5}_{-2.4}(\text{stat}) \pm 1.1(\text{syst}) \text{ pb}$ and $\sigma_{WW} = 12.6^{+3.2}_{-3.0}(\text{stat}) \pm 1.3(\text{syst}) \text{ pb}$, $\sigma_{Z \rightarrow \tau\tau} = 233^{+45}_{-42}(\text{stat}) \pm 17(\text{syst}) \text{ pb}$ for the two fitted background cross sections, which are in good agreement with the theoretical expectations[9].

2.2 Lepton plus jets channel

The lepton + jets signature represents the golden channel for top cross section (and mass) measurements. It benefits from high lepton trigger efficiency combined with large branching fraction (almost 30% for e/ μ plus jets) but suffers from higher background with respect to the dilepton

channel. The most significant background contribution is from $W + jets$ events, important are also multi-jet events with one jet misidentified as a lepton, diboson and single top production. These backgrounds can be estimated by fitting kinematic distributions like the total transverse energy or/and reduced by requiring at least one jet to be b -tagged ($S/B \sim 2 - 4$ with single tagging and $S/B > 10$ with double tagging). Different tagging algorithm have been developed at Tevatron[5]. The secondary vertex tagger and the jet probability tagger exploit the capabilities of the silicon microstrip detectors to reconstruct tracks displaced with respect to the primary vertex. The soft lepton tagger identifies the soft muon from the semileptonic b -decay.

Both CDF and D \emptyset collaborations performed counting experiment measurements applying secondary vertex taggers. These analyses, performed with 320 pb^{-1} and 365 pb^{-1} for CDF and D \emptyset respectively, represent right now the most precise $t\bar{t}$ cross section measurements, each with a total uncertainty close to 15%. Events are selected by requiring one (and only one) isolated high- p_T electron or muon, $\cancel{E}_T > 20 \text{ GeV}$ and three or more jets with $E_T > 15 \text{ GeV}$ (with $|\eta| < 2$ at CDF and with $|y| < 2.5$ at D \emptyset), lower jet multiplicity events are still used to check the background estimations. The dataset selected above is dominated by real W bosons with associated light flavor production, a background that can be strongly suppressed by requiring at least one b -jet in the event. The sample also includes contributions from multi-jet events in which a jet is misidentified as an electron or in which a muon originating from the semileptonic decay of a heavy quark appears isolated. In addition, significant \cancel{E}_T can arise from fluctuations and mismeasurements of the jet energies. The estimation of the sample composition is based both on Monte Carlo simulations and data and represents one of the main sources of systematic uncertainty together with the uncertainty on the b -tagging and the lepton reconstruction efficiency. To measure the cross section D \emptyset performed a fit to eight different channels: $e/\mu+jets$ with 3 or ≥ 4 jets and with one or two or more tags. The result is: $\sigma_{t\bar{t}} = 8.1^{+1.3}_{-1.2}(\text{stat+syst}) \pm 0.5(\text{lumi}) \text{ pb}$ (Fig. 4). CDF measured the cross section in the one (and more) and two (and more) tags samples obtaining respectively: $\sigma_{t\bar{t}} = 8.9 \pm 0.9(\text{stat})^{+1.2}_{-0.9}(\text{syst}) \text{ pb}$ and $\sigma_{t\bar{t}} = 10.4^{+1.6}_{-1.4}(\text{stat})^{+2.1}_{-1.4}(\text{syst}) \text{ pb}$.

Another analysis performed at D \emptyset exploits only the kinematic properties of the events to separate signal from background, with no use of the b-tagging requirements. To extract the fraction of $t\bar{t}$ events in the sample a discriminant function has been constructed. This function makes use of the differences between the kinematic properties of the $t\bar{t}$ events and the backgrounds. The variables have been selected in order to provide the best separation between signal and background and the least sensitivity to the jet energy calibration which in the end represents the 90% of the total systematic uncertainty. The measurement of the $t\bar{t}$ cross section has been performed (230 pb^{-1}) in each lepton channel separately and then combined yielding: $\sigma_{t\bar{t}} = 6.7^{+1.4}_{-1.3}(\text{stat})^{+1.6}_{-1.1}(\text{syst}) \pm 0.4(\text{lumi}) \text{ pb}$ (Fig. 5).

An innovative approach the lepton+jets channel is actually to look at the events with *no* reconstructed lepton in the data sample collected by the multi-jet trigger designed for the all-hadronic top analyses. The $\cancel{E}_T + jets + b$ -tags analysis performed at CDF in fact rejects events with a good, high- p_T electron or muon to avoid overlaps with the other lepton+jets analyses. The aim is to recover part of $e/\mu + jets$ sample with undetected lepton but especially to include $\tau + jets$ events by requiring significant \cancel{E}_T and exploiting the geometrical properties to discriminate the quark pair production from background processes. The event selection requires four or more jets ($E_T \geq 15 \text{ GeV}$) with at least one b -tag, large missing transverse energy significance ($\cancel{E}_T / \sqrt{\sum E_T} \geq 4 \text{ GeV}^{1/2}$) and large

total transverse energy ($\sum E_T^{jets} > 125\text{GeV}$). To suppress the multijet contamination the \cancel{E}_T is required not to be aligned with the jets directions ($\Delta\Phi(\cancel{E}_T, jets) \geq 0.4\text{rad}$). Background contribution yields are estimated from the data. The cross section measurement then is performed by counting tagged jets in the $4 \leq N_{jet} \leq 8$ sample. The measured cross section value in a 310 pb^{-1} data sample is found to be: $\sigma_{t\bar{t}} = 6.1 \pm 1.2(\text{stat})^{+1.4}_{-1.0}(\text{syst})\text{ pb}$ (Fig. 6).

2.3 All hadronic channel

The all hadronic channel provides a very large event sample (branching fraction $\sim 45\%$) and allows to fully reconstruct the $t\bar{t}$ system. Nevertheless it is the most challenging due to the overwhelming multi-jet QCD background. After a specifically designed trigger the signal to noise ratio is about $1 : 3000$; the bulk of the background is rejected by the requirement of at least one identified $b - jet$ in the event and further suppressed by cutting on a set of kinematical and event shape variables.

In the CDF analysis the kinematical requirements aim to maximize the $S/\sqrt{B+S}$ by applying selections on the number of jets, the total transverse energy, the centrality, the aplanarity and the sub-leading energy ($\sum_3 E_T \equiv \sum E_T - E_T^1 - E_T^2$) obtained by removing the two jets with the highest E_T . After these requirements and the request for at least one $b - jet$ the signal to noise of the sample increases to about $1 : 5$. The cross section measurement is then performed by counting $b - tags$ in the events with 6 to 8 jets. On a data sample of 310 pb^{-1} the measurement for the cross section is: $\sigma_{t\bar{t}} = 8.0 \pm 1.8(\text{stat})^{+3.5}_{-2.4}(\text{syst})\text{ pb}$ (Fig. 7).

In the D \emptyset analysis the kinematical selection is implemented via an artificial neural net (ANN). After optimization, six variables have been chosen to discriminate signal from background. The selection of the set of variables is driven by the requirement that the expected statistical significance of the cross section should stay comparable to when a larger number of input variables is used. Also, the usage of variable that are known to be highly dependent on the jet energy has been limited as much as possible since uncertainties in the jet energy calibration are by far the largest source of systematic uncertainty in the all hadronic channel. The final selection to enrich the sample in $t\bar{t}$ signal is applied by cutting on the ANN discriminant output ($D > 0.9$). The $t\bar{t}$ cross section measurement is then performed as a counting experiment and in a data sample of 350 pb^{-1} yields: $\sigma_{t\bar{t}} = 5.2^{+2.6}_{-2.5}(\text{stat})^{+1.5}_{-1.0}(\text{syst}) \pm 0.3(\text{lumi})\text{ pb}$ (Fig. 8).

3. Resonant $t\bar{t}$ production search

The very large top quark mass suggests that it may play a special role in the dynamics of the electroweak symmetry breaking. One of the various models incorporating this possibility is topcolor where the large top quark mass can be generated through a dynamical $t\bar{t}$ condensate, X, which is formed by a new strong gauge force preferentially coupled to the third generation of fermions. In one particular model, topcolor-assisted technicolor, X couples weakly to the first and the second generations and strongly to the third generation of quarks, and has no coupling to leptons. CDF and D \emptyset collaborations performed model independent searches for a narrow-width heavy resonance X decaying into $t\bar{t}$, only the lepton+jets final state has been considered.

The CDF approach is to use matrix element information to help with the $M_{t\bar{t}}$ reconstruction. Its basic idea is to use the theoretical differential cross section of the considered process as an

input for the event reconstruction and is particular suitable for topologies with missing (neutrino) or degraded (jets) information. The a priori probability density for producing a particular $t\bar{t}$ parton level final state $\{\vec{p}\}$ *relative to other final states* is simply its normalized differential cross section, denoted by $P_1(\{\vec{p}\})$. The apriori probability density for the parton level final state $\{\vec{p}\}$ *and* the measured jet quantities $\{\vec{j}\}$ is given by the product $P_2(\{\vec{p}\}, \{\vec{j}\}) = P_1(\{\vec{p}\}) \cdot T(\vec{j}_1|\vec{p}_1) \cdot T(\vec{j}_2|\vec{p}_2) \cdot T(\vec{j}_3|\vec{p}_3) \cdot T(\vec{j}_4|\vec{p}_4)$ where the $T(\vec{j}_i|\vec{p}_i)$ denote the parton to jet *transfer function*, i.e. the probability that a parton of momentum $\{\vec{p}\}$ is measured as a jet of momentum $\{\vec{j}\}$. From $P_2(\{\vec{p}\}, \{\vec{j}\})$ one can build $P(\{\vec{p}\}|\{\vec{j}\})$, the posterior probability of having the parton momenta $\{\vec{p}\}$ *given* the observed quantities $\{\vec{j}\}$. Having that distribution it is possible to derive probability distribution for any other variable function of $\{\vec{p}\}$, in particular $M_{t\bar{t}}$; the mean of such distribution is finally defined as the reconstructed $M_{t\bar{t}}$ value for the event. The reconstruction algorithm shows excellent performances when the parton are correctly associated to the jets; when applied to resonance sample events with incorrectly jet association a low mass shoulder in the $M_{t\bar{t}}$ distribution is created, reducing the overall resolution on the signal reconstruction. Finally, the $M_{t\bar{t}}$ spectrum for the data (320 pb^{-1}) has been reconstructed and fit for the presence of resonant $t\bar{t}$ contamination. Ten different resonance mass hypothesis from 450 to 900 GeV/c^2 has been tested and for each of them a 95% C.L. upper limit has been calculated since no evidence for the signal has been found (Fig. 10).

The D \emptyset collaboration performed the analysis using a constrained kinematic fit to reconstruct the $t\bar{t}$ invariant mass. This recipe has been successfully used in Run I for the top quark mass measurement. The following constraints are used in the fit: two jets must form the invariant mass of the W boson ($M_W = 80.4 \text{ GeV}/c^2$), the lepton and the \cancel{E}_T , taking into account the longitudinal momentum of the neutrino, must form the invariant mass of the W boson, the masses of the reconstructed top quarks have to be equal, and are set to $M_t = 175 \text{ GeV}/c^2$. Only the four highest p_T jets are considered in the kinematic fit. From the resulting twelve possible jet-parton assignments, the one with the lowest χ^2 is chosen. This is found to give the correct solution in about 65% of the $t\bar{t}$ events. Finally, the $M_{t\bar{t}}$ spectrum for the data (365 pb^{-1}) has been reconstructed and fit for the presence of resonant $t\bar{t}$ contamination. Ten different resonance mass hypothesis from 350 to 1000 GeV/c^2 has been tested and for each of them a 95% C.L. upper limit has been calculated (Fig. 11).

4. Summary and Conclusions

In this article measurements of the top pair production cross section at Tevatron were presented. All the measurements from both CDF and D \emptyset experiments are consistent with each other and with the Standard Model prediction (Fig. 9). A search for a narrow resonance decaying to $t\bar{t}$ has also been reviewed. As the amount of Run II data collected increases and the systematic uncertainties determined from data decreases, the Tevatron experiments will be able to achieve even more precise measurements of the top properties and probe for physics beyond the Standard Model.

5. Acknowledgments

I would like to thank the organizers for this very enjoyable conference and their hospitality. I must also acknowledge my CDF and D \emptyset colleagues whose work went into the results presented here.

References

- [1] F. Abe *et al.* [CDF Collaboration], Phys. Rev. Lett. **74**, 2626 (1995) [arXiv:hep-ex/9503002].
S. Abachi *et al.* [D0 Collaboration], Phys. Rev. Lett. **74**, 2632 (1995) [arXiv:hep-ex/9503003].
- [2] C.T. Hill Phys. Lett. B **345**, 483 (1995); C.T. Hill and S.J. Parke, Phys. Rev. D **49**, 4454 (1994)
- [3] R.M. Harris, C.T. Hill, and S.J. Parke, Fermilab Report No. Fermilab-FN-687; hep-ph/9911288, 1999
- [4] Proceedings from this conference. K. Hatakeyama, “How to calibrate Jet Energy scale”.
- [5] Proceedings from this conference. C. Neu, “How to estimate b-tag efficiency and false positive rate”.
- [6] D. Acosta *et al.*, (CDF Collaboration), Phys. Rev. D **71**, 032001 (2005).
- [7] V. Abazov *et al.*, (D \emptyset Collaboration), Submitted to Nucl. Intrum. Methods Phys. Res. A (2005).
- [8] CDF and D \emptyset use cylindrical coordinate systems with the z axis along the proton beam axis.
Pseudorapidity is $\eta \equiv -\ln(\tan(\theta/2))$, where θ is the polar angle, while
 $p_T = |p| \sin(\theta)$, $E_T = E \sin(\theta)$. The rapidity is $y = \frac{1}{2} \ln \frac{E+p_z}{E-p_z}$.
- [9] J. M. Campbell and R. K. Ellis, Phys. Rev. D **60**, 113006 (1999) [arXiv:hep-ph/9905386].
R. Hamberg, W. L. van Neerven and T. Matsuura, Nucl. Phys. B **359**, 343 (1991)
J. Pumplin, D. R. Stump, J. Huston, H. L. Lai, P. Nadolsky and W. K. Tung, JHEP **0207**, 012 (2002)
[arXiv:hep-ph/0201195].
D. Stump, J. Huston, J. Pumplin, W. K. Tung, H. L. Lai, S. Kuhlmann and J. F. Owens, JHEP **0310**, 046 (2003) [arXiv:hep-ph/0303013].

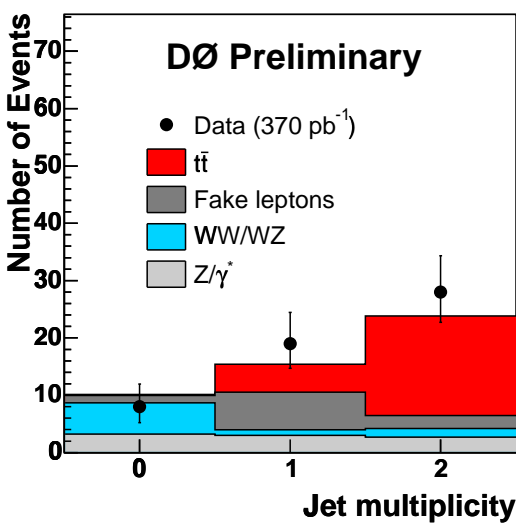


Figure 2: D \emptyset $t\bar{t}$ cross section measurement in the dilepton channel. Observed and predicted number of events with 0, 1 and 2 or more jets.

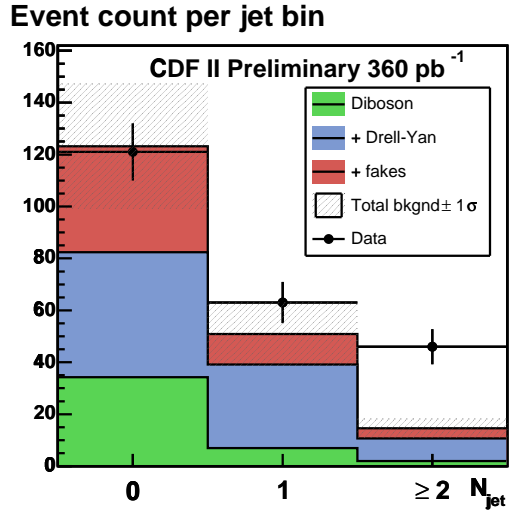


Figure 3: CDF $t\bar{t}$ cross section measurement in the lepton+track analysis. Predicted and observed number of events as a function of jet multiplicity for oppositely charged leptons.

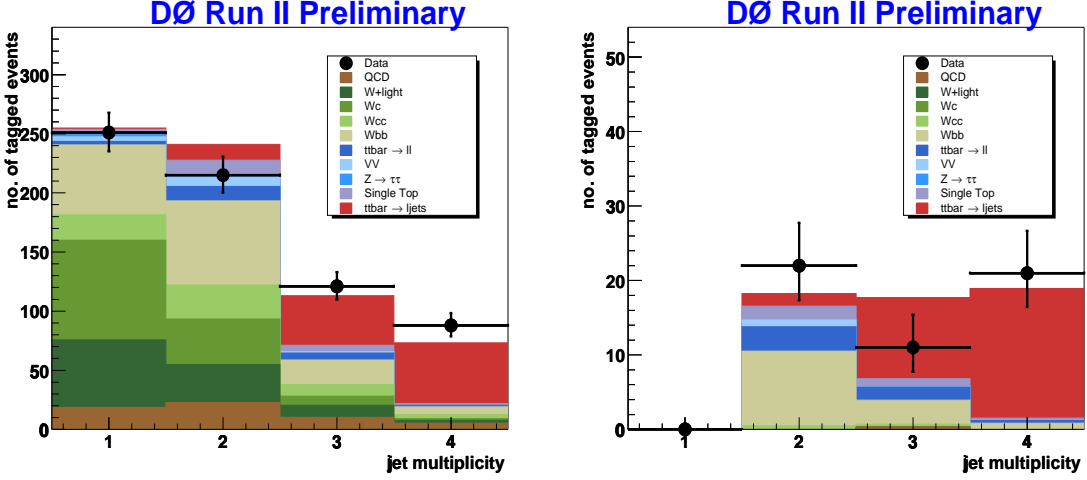


Figure 4: DØ $t\bar{t}$ cross section measurement using b -tagging in the lepton+jets channel. Predicted and observed tagged events in 365pb^{-1} of data: single tags (left) and double tags (right).

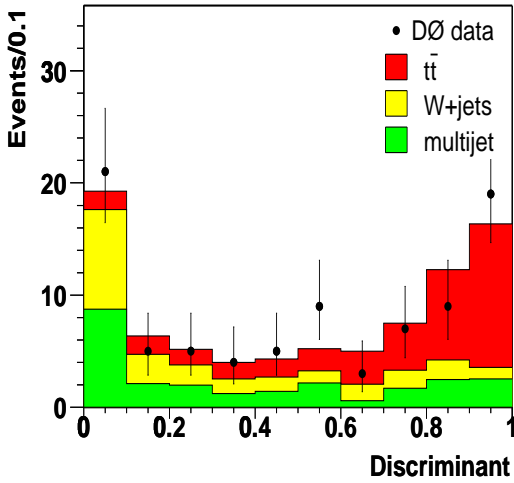


Figure 5: DØ $t\bar{t}$ cross section measurement in the $\ell+jets$ channel. Likelihood discriminant distribution for data overlaid with the result of the fit of $t\bar{t}$, $W+jets$ and multijet backgrounds.

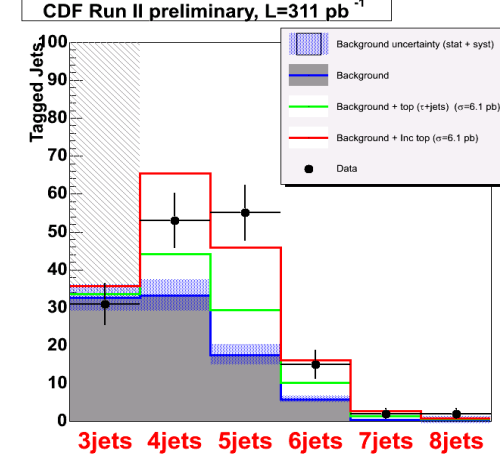


Figure 6: CDF $\ell_T + \text{jets}$ analysis. Tagging background predictions after kinematical selections. The predicted number of positive tags as a function of the jet multiplicity is shown for background, together with the contribution from $t\bar{t} \rightarrow \tau + jets$ and inclusive Monte Carlo events. Points refers to the observed tagged jet in the data.

POS(TOP2006)008

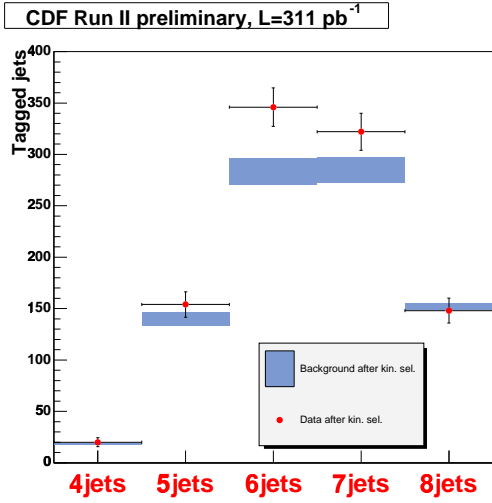


Figure 7: CDF all-hadronic analysis. Comparison between tags expected from background contributions and observed tags in each multiplicity bins.

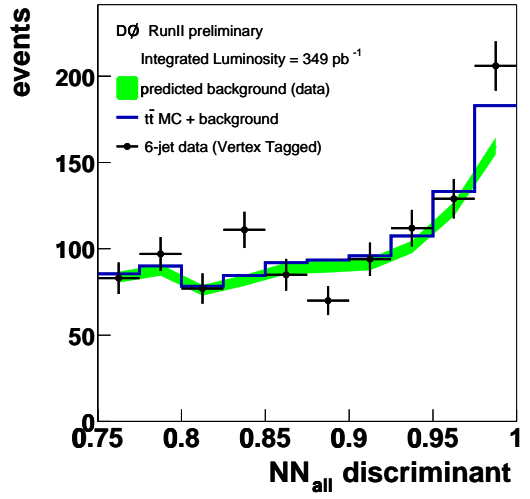


Figure 8: D0 all-hadronic analysis. Output of the NN. The last four bins include all the data that pass all the cuts included the $D_{NN} > 0.9$ cut. Shown is the tagged data (points), the prediction for the background (green band) and the $t\bar{t}$ to all-hadronic Monte Carlo added to it (blue histogram, a cross section of 6.5 pb is assumed).

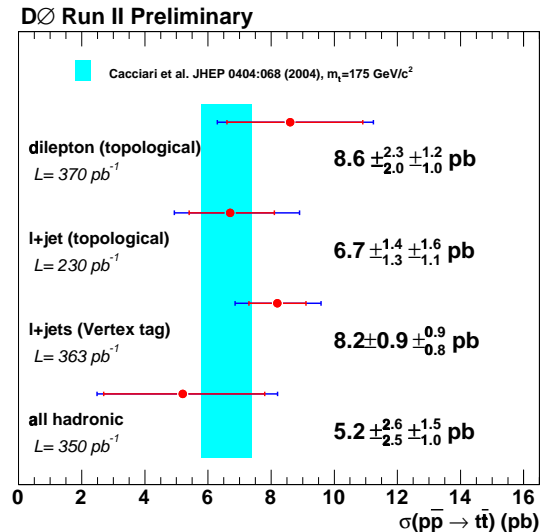
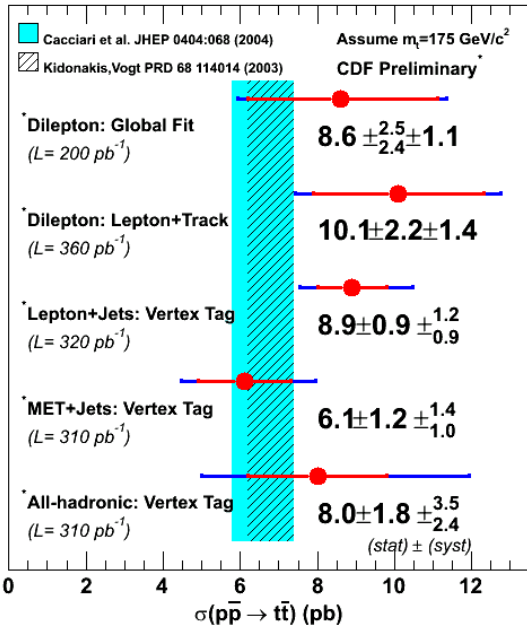


Figure 9: Summary of top pair production experimental results from CDF (left) and D0 (right) experiments. The bands represent the NLO theory calculation for a $175 \text{ GeV}/c^2$ top mass.

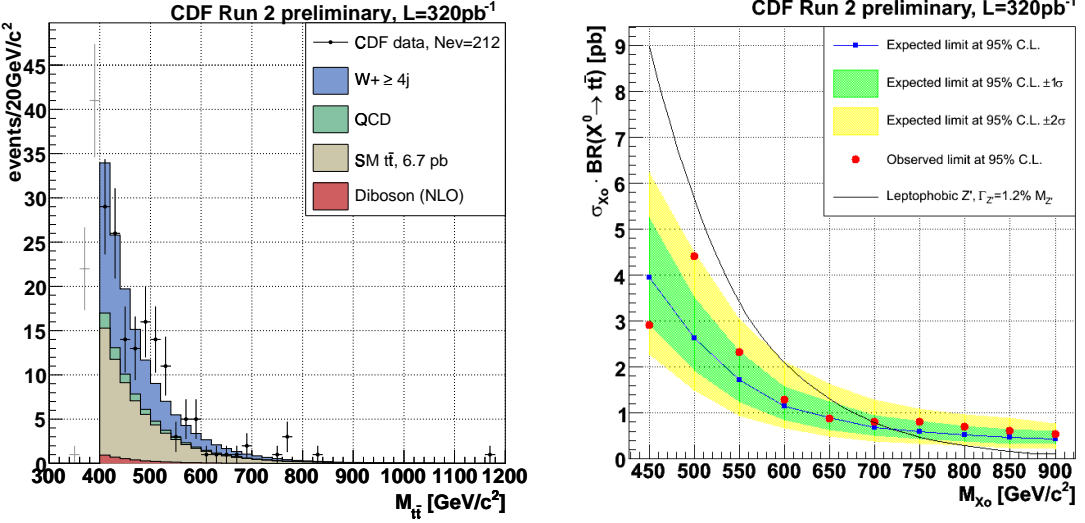


Figure 10: CDF resonant $t\bar{t}$ search. Left: reconstructed $M_{t\bar{t}}$ spectrum vs the standard model expectation in the search region above the $400\text{ GeV}/c^2$ cut. Grey points show data distribution below $400\text{ GeV}/c^2$. Right: expected and experimental upper limits for a resonance in 320 pb^{-1} of CDF data together with leptophobic topcolor Z' cross section prediction. Green and yellow areas define the central 68% and 95% frequentistic bands for the expected limits.

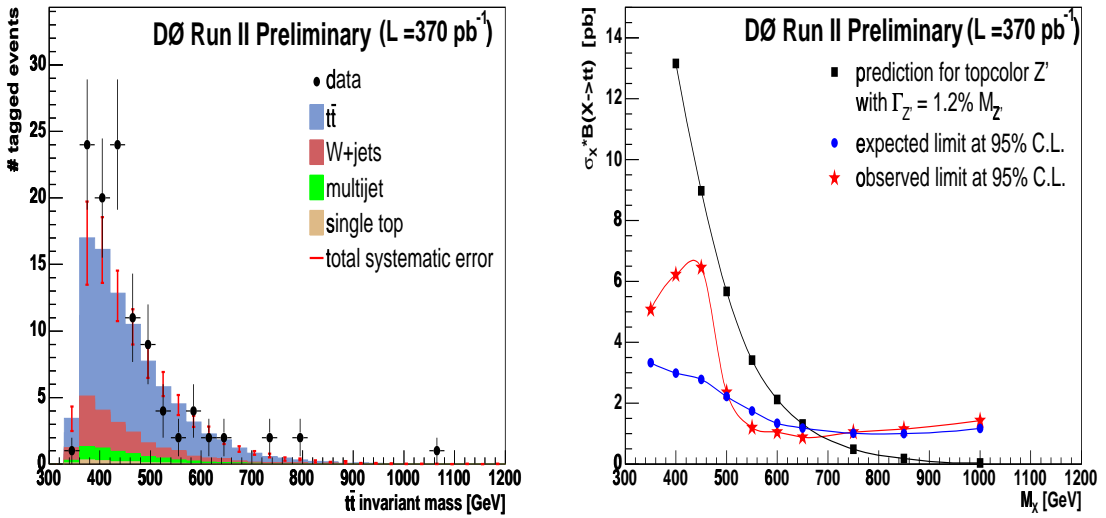


Figure 11: DØ resonant $t\bar{t}$ search. Left: resulting mass distribution for the combined ℓ +jets channels. The error bars on top of the Standard Model background indicate the total systematic uncertainty, which has significant bin-to-bin correlations. Right: Expected and observed 95% C.L. upper limits on $\sigma_X \cdot Br(X \rightarrow t\bar{t})$ compared with the predicted topcolor-assisted technicolor cross section for a Z' boson with a width of $\Gamma_{Z'} = 0.012M_{Z'}$ as a function of resonance mass M_X .